Earth and Planetary Science Letters 385 (2014) 130–136

Contents lists available at ScienceDirect

Earth and Planetary Science Letters

www.elsevier.com/locate/epsl

Iron spin state in silicate glass at high pressure: Implications for melts in the Earth's lower mantle

C. Prescher [a,*], C. Weigel [b], C. McCammon [a], O. Narygina [c], V. Potapkin [a,d], I. Kupenko [a,d], R. Sinmyo [a], A.I. Chumakov [c], L. Dubrovinsky [a]

[a] Bayerisches Geoinstitut, Universität Bayreuth, D-95440 Bayreuth, Germany
[b] CNRS, Laboratoire Charles Coulomb UMR 5221, F-34095, Montpellier, France
[c] PANalytical B.V., Lelyweg 1 (7602 EA), PO Box 13, 7600 AA Almelo, Netherlands
[d] European Synchrotron Radiation Facility, BP 220, F-38043 Grenoble, France

ARTICLE INFO

Article history:
Received 6 November 2012
Received in revised form 2 September 2013
Accepted 23 October 2013
Available online 12 November 2013
Editor: T. Elliott

Keywords:
lower mantle
Mössbauer spectroscopy
glass
spin crossover

ABSTRACT

We report a Mössbauer spectroscopic study of a Fe^{2+}-rich aluminous silicate glass and a Fe^{3+}-rich sodium silicate glass measured in a diamond anvil cell up to 84 GPa. The hyperfine parameters vary smoothly with pressure and are consistent with a gradual increase in coordination number with pressure. Fe^{2+} and Fe^{3+} remain in the high-spin state and show no evidence of spin crossover over the measured pressure range. A spin crossover may eventually occur at higher pressures; however the strong thermal broadening of the crossover region due to Boltzmann statistics would prevent any spin crossover from occurring sharply at P,T conditions down to the base of the lower mantle. Our results in combination with recent solid/melt partitioning data in a chondritic system imply that strong preferential partitioning of iron into the melt phase cannot give rise to negatively buoyant melts in the Earth's lower mantle.

1. Introduction

The physical properties of melts in the Earth's mantle have a fundamental influence on the chemical and thermal evolution of the Earth. Especially the density contrast between solid and melt is a major factor affecting chemical stratification during an early magma ocean after the moon-forming impact (Tonks and Melosh, 1993; Agnor et al., 1999). At low pressure melt densities are usually smaller than the density of the corresponding solids, resulting in a buoyant melt ascending to the Earth's surface. However, experiments have shown that ultramafic melts become denser than the surrounding solids in the upper mantle, while in the transition zone this density relationship is reversed (Rigden et al., 1984; Agee and Walker, 1988; Miller et al., 1991). For the lower mantle, extrapolation of low pressure experiments suggests that density crossovers between solids and melts will also occur near the core mantle boundary (CMB) (Ohtani and Maeda, 2001). In support of this suggestion Williams and Garnero (1996) have proposed stable partial melts at the CMB as a possible explanation of seismological data.

In principle there are two mechanisms for melts becoming denser than solids. The first mechanism is by faster densification of the melt network with pressure, e.g., coordination changes occurring in a melt at lower pressure than in the solid, while the second mechanism is by preferential partitioning of heavier elements into the melt. The first mechanism has been suggested to occur at the base of the Earth's lower mantle for $MgSiO_3$ melt (Murakami and Bass, 2011), whereas first-principle molecular dynamics calculations (Stixrude and Karki, 2005; De Koker et al., 2013) indicate that a density crossover only occurs in Fe-bearing systems near the CMB, suggesting a combination of both mechanisms. Recently Nomura et al. (2011) proposed the preferential partitioning mechanism to occur at lower pressures in the mid part of the lower mantle based on experiments in an olivine composition $(Mg_{0.89}Fe_{0.11})_2SiO_4$. They observed a sharp discontinuity in the pressure dependence of the Fe/Mg solid/melt partition coefficient at 76 GPa, resulting in a strong enrichment of Fe in the melt, which would produce a denser negatively buoyant melt. The sharp discontinuity was explained by an iron spin crossover seen in their X-ray emission spectroscopy (XES) data collected on $(Mg_{0.95}Fe_{0.05})SiO_3$ glass during room temperature compression.

* Corresponding author. Present address: Center for Advanced Radiation Sources, University of Chicago, Chicago, IL, 60439, USA.
E-mail address: clemens.prescher@gmail.com (C. Prescher).

0012-821X/$ – see front matter
http://dx.doi.org/10.1016/j.epsl.2013.10.040

However, Andrault et al. (2012) reported a much lower degree of iron enrichment in silicate melt based on partitioning experiments at liquidus temperatures on a (Ca, Mg, Al, Si, Fe) oxide glass with chondritic composition, resulting in a melt that would be lighter than the surrounding mantle and hence would segregate upwards.

In order to reconcile the difference between the results of Nomura et al. (2011) and Andrault et al. (2012), it is important to understand the electronic behavior of iron in both glass and melt as a function of composition. Partitioning experiments can only provide an indirect indication of the iron spin state, while a more direct determination comes from a method such as Mössbauer spectroscopy, which is a sensitive probe for detecting structural and spin changes in Fe-bearing materials. Direct investigation of iron spin states in silicate melts at high pressures and high temperatures using Mössbauer spectroscopy is beyond current experimental capabilities; however, silicate glasses can be used as structural analogues for melts in the Earth's lower mantle.

In this paper we present a Mössbauer spectroscopic study of a Fe^{2+}-rich and a Fe^{3+}-rich silicate glass measured *in situ* in a diamond anvil cell at pressures up to 84 GPa. We investigate the effect of pressure on the hyperfine parameters of these silicate glasses and determine whether spin crossover occurs, and then apply our results to the behavior of silicate melts at lower mantle conditions.

2. Experimental details

The mainly Fe^{3+}-bearing $(Na_{0.98}Fe_{1.04})Si_{2.05}O_6$ (NaFe-silicate) and Fe^{2+}-bearing $(Mg_{0.823}Fe_{0.135})(Al_{0.057}Si_{0.982})O_3$ (MgFeAl-silicate) glasses were prepared from stoichiometric mixtures of dried, reagent grade oxides of Na_2CO_3, $MgCO_3$, Al_2O_3, SiO_2, and $^{57}Fe_2O_3$ (95.86% ^{57}Fe). The powdered mixtures were decarbonated at 750 °C for 12 h in platinum crucibles. The starting material of NaFe-silicate glass was melted at 1100 °C in an electric furnace in air for 2 h. The temperature was then brought to 1300 °C for 2 h and finally to 1450 °C for 30 min. The melts were quenched by rapid immersion of the bottom of the crucible in water, ground to a powder and re-melted with the same cycle. This grinding–melting process was repeated three times to ensure good chemical homogeneity. Transmission electron microscope images confirmed the absence of nanometer-sized heterogeneities in the MgFeAl-silicate glass and its composition was determined using an electron microprobe. The starting material of MgFeAl-silicate glass was melted at 1600 °C in a Fe-saturated platinum crucible for 4 h and quenched by rapid immersion in a crucible of water. The ground glass was then reduced in a gas-mixing furnace in a H_2–CO_2 atmosphere at 700 °C and $\log fO_2 = -21$ for 1 h. The composition of the resulting MgFeAl-silicate glass was determined using an electron microprobe and no inhomogeneity was observed within the resolution of the measurements.

Diamond anvil cells with diamond culet sizes of 250 µm and a rhenium gasket with a 120 µm diameter hole were employed. The fluorescence of ruby chips (Mao et al., 1986) was used to estimate pressure before and after each measurement, whereby the error in pressure was calculated from the difference of both values.

We ran three experimental series: (1) MgFeAl-silicate glass with neon as pressure transmitting medium measured on compression up to 83 GPa, (2) NaFe-silicate glass without pressure transmitting medium measured on compression and decompression up to 56 GPa, and (3) NaFe-silicate glass with neon as pressure transmitting medium measured on compression up to 84 GPa. For neon gas loading the method of Kurnosov et al. (2008) was employed.

Mössbauer spectra of MgFeAl-silicate glass from experimental series (1) were collected using the recently developed Synchrotron Mössbauer Source (SMS) (Potapkin et al., 2012) at the Nuclear Resonance beamline (ID18) (Rüffer and Chumakov, 1996) at the European Synchrotron Radiation Facility (Grenoble, France). SMS spectroscopy enables the collection of energy domain Mössbauer spectra of small samples with relatively low iron concentrations on a timescale of only minutes, compared to days of collection time using a conventional radioactive Mössbauer source. Mössbauer spectra of NaFe-silicate glass from experimental series (2) and (3) were recorded at room temperature in transmission mode on a constant acceleration Mössbauer spectrometer with a nominal 370 MBq ^{57}Co high specific activity source in a 12-µm-thick Rh matrix. The velocity scales for all series were calibrated relative to a 25-µm-thick natural α-Fe foil and center shift values are given relative to α-Fe. MgFeAl-silicate glass spectra were fitted using a full transmission integral with a normalized Lorentzian-squared source lineshape (Potapkin et al., 2012) to accommodate for the difference in Mössbauer source properties and beam intensity of SMS compared to conventional Mössbauer spectroscopy. The SMS linewidth was controlled before and after each sample measurement using $K_2Mg^{57}Fe(CN)_6$. NaFe-silicate glass spectra were fitted in the thin absorber approximation. All spectra were fitted using the extended Voigt based fitting method (xVBF) (Lagarec and Rancourt, 1997) as implemented in the MossA software package (Prescher et al., 2012).

3. Results

Fig. 1(a) shows selected Mössbauer spectra and Fig. 1(b) shows the variation in center shift (CS) and quadrupole splitting (QS) with pressure of MgFeAl-silicate glass in Ne. The asymmetry in the height and width of the two peaks can be explained by a correlation between the CS and the QS. This correlation can be successfully fitted using the xVBF method (Lagarec and Rancourt, 1997), which was especially developed for disordered systems such as glasses. In the xVBF approach Gaussian distributions of CS and QS are utilized, whereby a linear correlation is allowed between the two parameters. The spectra were fitted using a Fe^{2+} doublet with xVBF CS–QS coupling between −0.5 and −0.6; see Lagarec and Rancourt (1997) for further details. The plotted values of CS and QS are the means of the Gaussian distributions of the respective parameters. The CS decreases almost linearly up to 50 GPa and stays constant up to 83 GPa; whereas the QS increases up to 30 GPa and stays constant at higher pressures up to 83 GPa. No evidence was found for the presence of Fe^{3+} within the uncertainty of the data.

Fig. 2 shows selected spectra of the NaFe-silicate glass measurements. The spectra are composed of an intense Fe^{3+} doublet and a weak Fe^{2+} doublet. The widths of the doublets of the NaFe-silicate glass compressed without pressure medium are highly broadened compared to those compressed with Ne as pressure transmitting medium. This is likely an effect of higher pressure gradients and stress within the sample chamber due to the absence of a pressure transmitting medium. This broadening was accounted for by modeling the Fe^{3+}-site with two Gaussian QS components, whereas the NaFe-silicate glass in Ne was modeled with only one QS component. The correlation between CS and QS of Fe^{3+} is close to zero for both sites in both experiments. Fig. 3 shows the variation of hyperfine parameters with pressure. The CS and QS values of NaFe-silicate glass with no pressure medium were calculated as the weighted average of the two Gaussian QS distributions. The QS for both Fe^{2+} and Fe^{3+} increases up to 15 GPa, it is nearly constant between 15 and 60 GPa, and it increases moderately above 60 GPa. The CS of Fe^{2+} and Fe^{3+} increases up to 15 GPa and then remains constant within experimental uncertainty up to 84 GPa.

The area of the Fe^{3+} absorption increases relative to the Fe^{2+} absorption in the NaFe-silicate glass with increasing pressure (Fig. 4). Although there are differences in values between the samples measured with and without pressure transmitting medium,

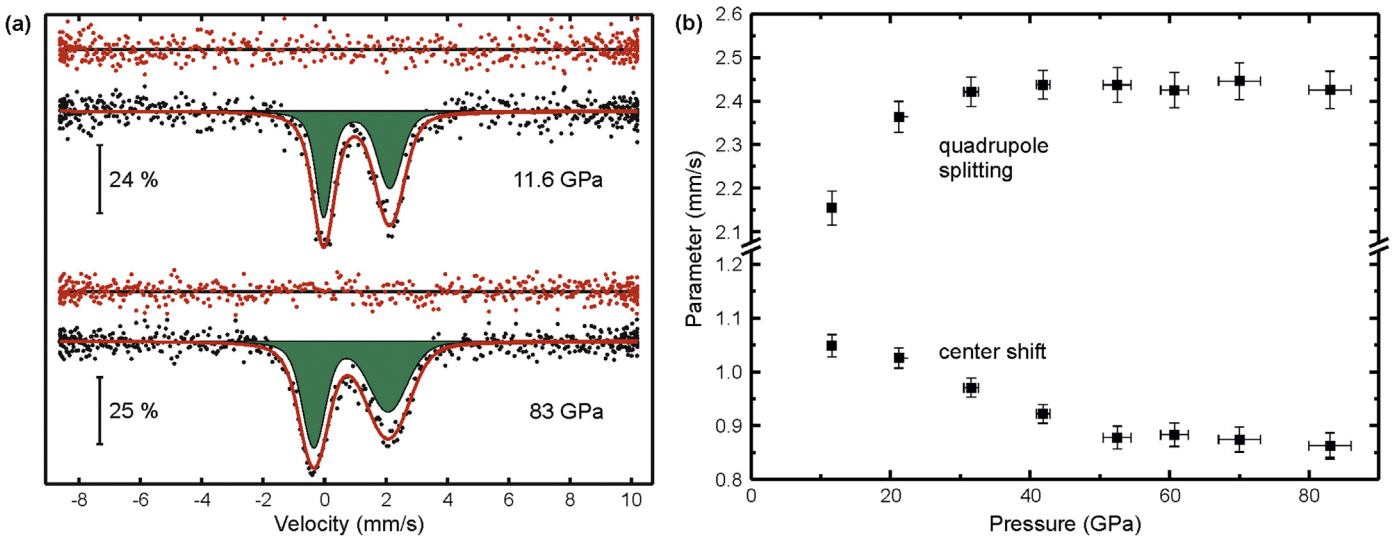

Fig. 1. (a) Selected Mössbauer spectra of MgFeAl-silicate glass. (b) Variation in center shift (CS) and quadrupole splitting (QS) of Fe^{2+} with pressure up to 83 GPa. Error bars are given as 2σ of the fitted parameters.

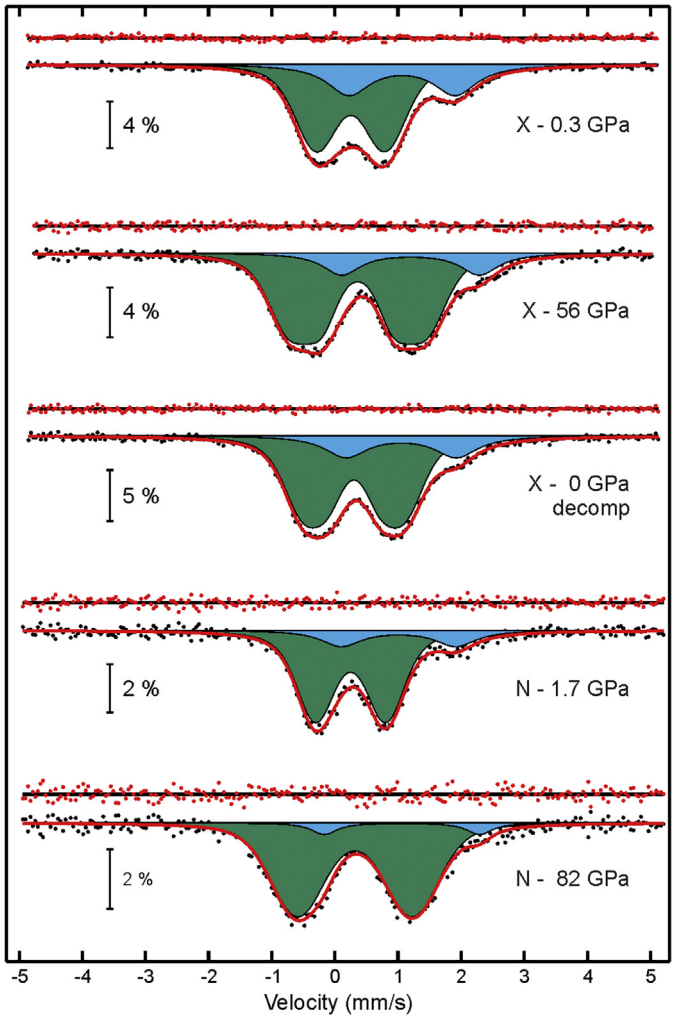

Fig. 2. Selected Mössbauer spectra of the NaFe-silicate glass. The upper three spectra are measured without pressure medium (X) and show (from top to bottom) the initial spectrum, the highest achieved pressure, and the spectrum after decompression. The lower two spectra are measured with neon as pressure transmitting medium (N) and show a spectrum at low and high pressure.

they are not significant and the overall trend is the same for all samples.

4. Discussion

At sufficiently high pressures, glasses typically adapt their atomic structure to compression by changing the coordination of the atoms and decreasing their polyhedral volumes. This behavior has two opposing effects on the CS of the corresponding Mössbauer doublet. CS is a measure of the difference in s-electron density at the nucleus between the source and the absorber, whereby the sign of the change in CS for a given change in s-electron density is determined by the sign of the relative change in the nuclear radius during the transition induced by the Mössbauer γ-ray. The excited state of ^{57}Fe is smaller than the ground state which means that CS decreases when the electron density at the nucleus increases. Pure compression of a coordination polyhedron will decrease CS with pressure, whereas a change to a higher coordination number typically increases CS, since the distance to the surrounding oxygen ions increases and consequently the electron density at the nucleus decreases.

The CS of Fe^{2+} in the MgFeAl-silicate glass and Fe^{2+} and Fe^{3+} in the NaFe-silicate glass behave differently with compression. In the NaFe-silicate glass the CS of the Fe^{3+} and the Fe^{2+} sites increases up to around 15 GPa and remains essentially constant up to the highest pressures achieved, which is consistent with a gradual increase in coordination number up to 15 GPa. On the other hand in the MgFeAl-silicate glass the CS of Fe^{2+} decreases up to 50 GPa and remains constant thereafter, which is consistent with a decreased interatomic distance up to 50 GPa. A similar trend has been observed for Fe^{2+} in amorphous $(Mg_{0.9}Fe_{0.1})_2SiO_4$ (Rouquette et al., 2008). However, according to the general predicted behavior of transition metals in silicate glasses under pressure, the Fe coordination number should increase with pressure (e.g., Keppler and Rubie, 1993). This suggests that while the average coordination number of Fe^{2+} in the MgFeAl-silicate glass increases with pressure, the compression of the polyhedron due to increased pressure has a stronger influence on the s-electron density, resulting in a net CS decrease with pressure. The constant value of CS above 50 GPa suggests that there may be a change in compression mechanism at this pressure, for example a change in the coordination number of Si from 4- to 6-fold. Results for SiO_2 and $MgSiO_3$ glass in the literature give two different transition pressures that have been estimated from experimental data

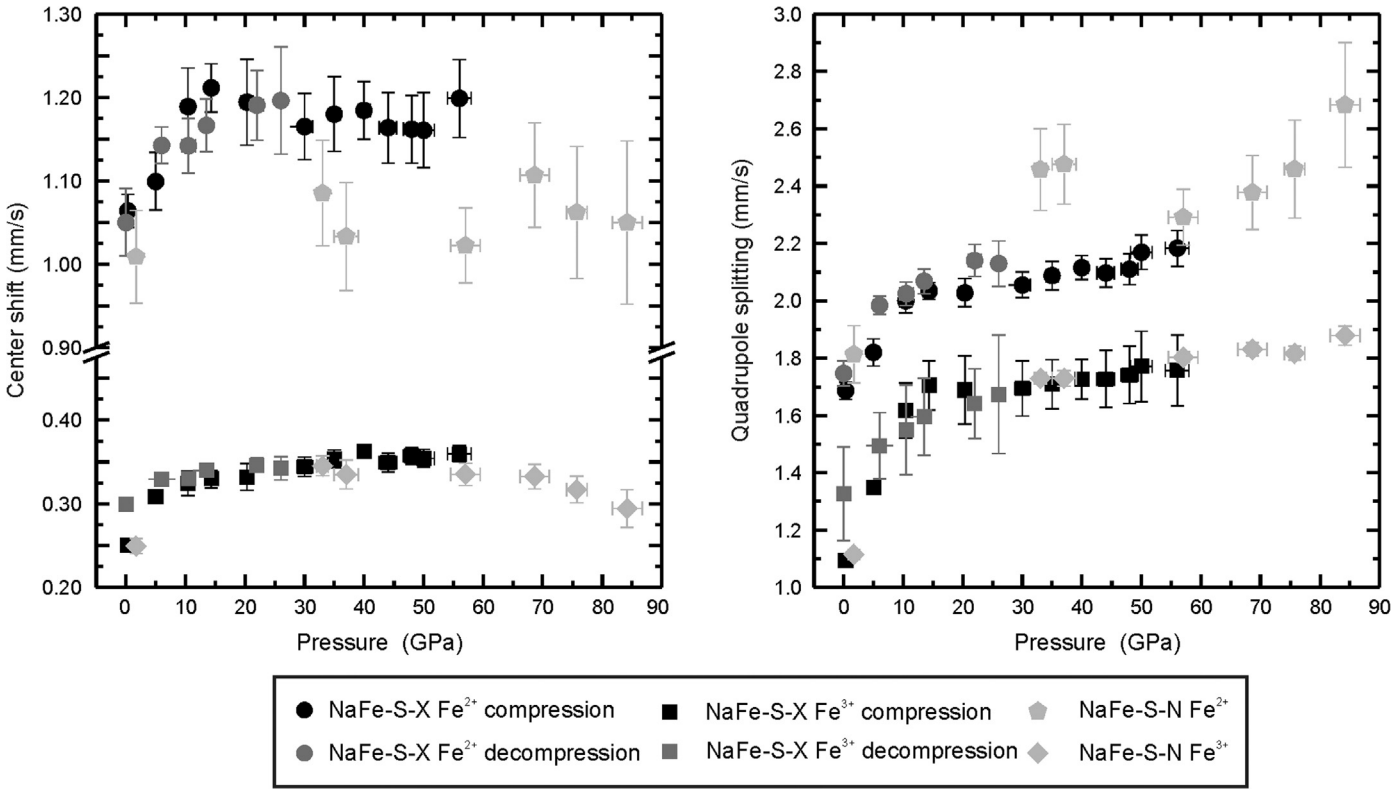

Fig. 3. Variation of center shift and quadrupole splitting for Fe^{2+} and Fe^{3+} with pressure of NaFe-silicate glass up to 84 GPa. The symbols refer to the different experimental series: "NaFe-S-X" denotes NaFe-silicate glass without pressure medium under compression for Fe^{2+} (black circles) and Fe^{3+} (black squares) and under decompression for Fe^{2+} (grey circles) and Fe^{3+} (grey squares), while "NaFe-S-N" denotes NaFe-silicate glass in neon pressure transmitting medium under compression for Fe^{2+} (grey pentagons) and Fe^{3+} (grey diamonds). Error bars are given as 2σ based on fitting statistics.

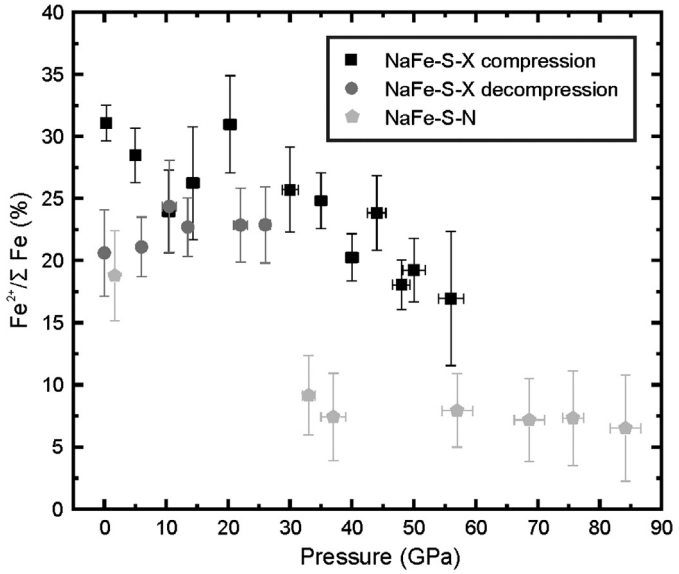

Fig. 4. Variation of $Fe^{2+}/\Sigma Fe$ with pressure of NaFe-silicate glass. The symbols refer to the different experimental series: "NaFe-S-X" denotes NaFe-silicate glass without pressure medium under compression (squares) and decompression (circles), while "NaFe-S-N" denotes NaFe-silicate glass in neon pressure transmitting medium under compression (pentagons). Error bars are given as 2σ based on fitting statistics.

obtained from different methods. Brillouin spectroscopy (Zha et al., 1994; Murakami and Bass, 2010, 2011), Raman spectroscopy (Shim and Catalli, 2009) and X-ray Raman scattering (Lin et al., 2007; Lee et al., 2008) give an estimate of 20–30 GPa, while X-ray diffraction measurements suggest that the density of SiO_2 glass approaches that of coesite around 40–50 GPa (Sato and Funamori, 2008; Funamori and Sato, 2010). The former methods likely indicate the onset of a gradual Si coordination change, while the latter method likely indicates the pressure at which most of the Si atoms are in 6-fold coordination in order to achieve a density similar to coesite. In addition molecular dynamic simulations of $MgSiO_3$ liquid show the absence of 4-fold-coordinated Si around 55 GPa (Stixrude and Karki, 2005). It is therefore reasonable to suggest that the change in slope of the CS with pressure around 50 GPa of Fe^{2+} in the MgFeAl-silicate glass is related to a change in Si coordination number from 4- to 6-fold.

Quadrupole splitting (QS) is a measure of the electric field gradient (EFG) acting on the nucleus. In the crystal field model the EFG can be expressed as the sum of a lattice term and a valence term (Ingalls, 1964). The lattice term arises from a deviation from cubic symmetry of the surrounding atoms in the crystalline lattice, while the valence term arises from an asymmetry in the charge distribution of the valence electrons. The QS is therefore affected by the valence state and the coordination environment as well as the distortion of the crystallographic site. The pressure dependence of the QS can be negative or positive, depending on the relative magnitude of the valence and lattice terms (e.g., McCammon, 2000). The QS of Fe^{2+} and Fe^{3+} in both glasses increases in the first 15–30 GPa and remains roughly constant up to the highest pressures achieved (similar to the behavior of Fe^{2+} in amorphous $(Mg_{0.9}Fe_{0.1})_2SiO_4$; Rouquette et al., 2008). The increase can be understood as an increased distortion of the coordination polyhedron, and the slope of the QS increase with pressure is similar to that seen in the QS pressure dependence of high-spin Fe^{2+} and Fe^{3+} in silicate perovskite (e.g., Li et al., 2006; Jackson et al., 2005; McCammon et al., 2008) and high-spin Fe^{2+} in magnesiowüstite (e.g., Lin et al., 2006).

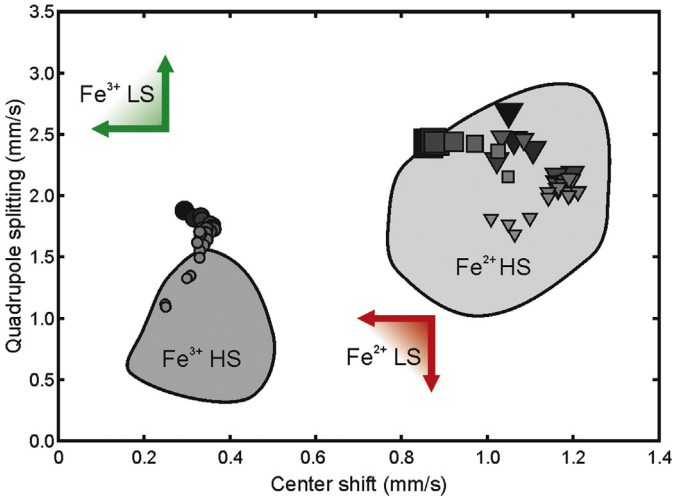

Fig. 5. Variation of center shift (CS) and quadrupole splitting (QS) for Fe^{2+} and Fe^{3+} in glasses. Symbols indicate results from this study, where symbol size and degree of darkness increase with increasing pressure. The shaded regions indicate values derived from Mössbauer spectra at ambient conditions of HS Fe^{2+} and HS Fe^{3+} in inorganic glasses (Dyar, 1985). The minimum changes of CS and QS during pressure induced HS to LS crossovers were calculated from the literature for Fe^{2+} (amorphous olivine – Rouquette et al., 2008; (Mg, Fe)O – Lin et al., 2006; silicate perovskite – Bengtson et al., 2009; Hsu et al., 2011, 2012) and Fe^{3+} (rare earth orthoferrites and $FeBO_3$ – Hearne et al., 1995; Xu et al., 2001; Sarkisyan et al., 2002; Pasternak et al., 2002; silicate perovskite – Bengtson et al., 2009; Catalli et al., 2010; Hsu et al., 2011, 2012) in order to estimate the corners of the regions where LS hyperfine parameters would be predicted to fall for the glasses in the current study (indicated in red and green for LS Fe^{2+} and LS Fe^{3+}, respectively). (For interpretation of the references to color in this figure legend, the reader is referred to the web version of this article.)

The change in relative area of the Fe^{3+} site over the Fe^{2+} site with pressure in the NaFe-silicate glass might be attributed to one or more of several effects. The first is a change of the recoil-free fractions of Fe^{2+} and Fe^{3+} relative to one another with increasing pressure. The recoil-free fraction, which is related to the mean-square displacement of the nucleus, could change differently with pressure for Fe^{3+} and Fe^{2+} due to differences in the change of the coordination environments. A second possibility is a pressure-induced oxidation of Fe^{2+}, either by reacting with residual oxygen adhering to the sample powder or by the disproportionation reaction $3Fe^{2+} \rightarrow 2Fe^{3+} + Fe^{0}$, forming small amounts of nanoparticle metallic iron that would not be easily detectable in the Mössbauer spectra. Without further information from other methods, it is not relevant to speculate about the origin of the change in relative areas, which can be a topic for further studies. Whatever the cause, however, the CS and QS hyperfine parameters of the Fe^{2+} and Fe^{3+} sites would not be affected, and therefore the conclusions drawn in this study remain the same.

The hyperfine parameters associated with the low-spin states of Fe^{2+} and Fe^{3+} in iron-bearing compounds generally differ significantly to their high-spin counterparts, providing a probe of spin crossover. CS and QS show a large decrease during HS–LS crossover of Fe^{2+} due to drastic changes in the shielding of the nucleus by *d*-electrons and the more symmetrical distribution of *d*-electrons in the LS state. During Fe^{3+} HS–LS crossover CS also decreases; however QS shows a large increase due to the loss of symmetry of the *d*-electron distribution. By comparing expected changes for HS to LS crossover of Fe^{2+} and Fe^{3+} with the measured hyperfine parameters in this study (Fig. 5) it is apparent that there is no evidence for spin crossover in either of the studied glasses. A similar conclusion was reached in a paper reporting an XES study of silicate glasses by Gu et al. (2012) which was published after the present paper was submitted.

Nomura et al. (2011) found evidence using XES for complete Fe^{2+} spin crossover in $Mg_{0.95}Fe_{0.05}SiO_3$ glass in a narrow pressure range from 59 to 77 GPa, while partial spin crossover of Fe^{2+} was found over a much larger pressure range in a pressure-induced amorphized sample of $(Mg_{0.9}Fe_{0.1})_2SiO_4$ (Rouquette et al., 2008). The higher iron concentration in the latter sample leads to enhanced iron–iron electronic exchange which stabilizes the high-spin state relative to the low-spin state (e.g., Kantor et al., 2009). We observed no Fe^{2+} spin transition in the MgFeAl-silicate glass up to 83 GPa, which can be understood through stronger iron–iron electronic exchange compared to amorphized $(Mg_{0.9}Fe_{0.1})_2SiO_4$ due to its higher iron concentration (Fe# = 0.14), and also larger interatomic distances due to substitution of the larger Al^{3+} for the smaller Si^{4+}. A similar argument can be applied to explain why no Fe^{3+} spin crossover is observed up to 84 GPa in the NaFe-silicate glass. The compositional effect is mainly the iron–iron electronic spin exchange interaction which has an opposing effect for Fe^{2+} and Fe^{3+}. It stabilizes high-spin Fe^{2+} over low-spin Fe^{2+} and low-spin Fe^{3+} over high-spin Fe^{2+}, due the absence of net spin in low-spin Fe^{2+} and high-spin Fe^{3+}. We therefore conclude that for higher Fe^{3+} concentrations, spin crossover should occur at lower pressures. Since the data do not show evidence for spin crossover in the glass with relatively high Fe^{3+} content, it is unlikely that spin crossover will occur in silicate glasses/melts with a lower Fe^{3+} concentration in this pressure range. Although spin crossover might eventually occur at higher pressures and temperatures, the strong thermal effect which increases the width of the crossover region according to Boltzmann statistics (e.g., Kantor et al., 2009) means that any spin crossover that occurred would not be sharp at P,T conditions down to the base of the lower mantle.

We observe no evidence for Fe^{3+} spin crossover in the NaFe-silicate glass up to 84 GPa, in contrast to reports in the literature for several other Fe^{3+}-rich oxides and silicates (Hearne et al., 1995; Xu et al., 2001; Pasternak et al., 2002; Sarkisyan et al., 2002; Bengtson et al., 2009; Catalli et al., 2010, 2011; Hsu et al., 2011, 2012). In those studies Fe^{3+} occupies a relatively undistorted octahedral site, for example Fe^{3+} in $ASiO_3$ perovskite undergoes an HS–LS crossover at ~50 GPa only when it occupies the octahedral B-site (Catalli et al., 2010, 2011; Hsu et al., 2011, 2012); whereas it remains in the HS state up to at least ~120 GPa when it occupies the 8–12-coordinated A-site (Catalli et al., 2010; Hsu et al., 2011, 2012). The coordination of Fe^{3+} in the NaFe-silicate glass at ambient pressure is 4- to 5-fold (Weigel et al., 2008). The increasing CS from 0 to 15 GPa suggests a gradual change to higher coordination number, although it is not possible to determine the exact coordination population of Fe^{3+} from Mössbauer spectroscopy. The absence of an HS–LS spin crossover of Fe^{3+} in the NaFe-silicate glass, however, suggests that Fe^{3+} coordination at high pressure differs from the highly symmetrical octahedral environment of the B-site in the perovskite structure. The crystal field splitting, a major driving factor for HS–LS crossover, is largest in an octahedral environment (e.g., Burns, 1993); hence a different coordination would increase the pressure of HS–LS crossover. To more accurately determine the coordination of Fe^{3+} in NaFe-silicate glass at high pressure requires further investigation with measurement methods such as EXAFS (Extended X-ray absorption fine structure) that are more diagnostic for coordination number.

Nomura et al. (2011) reported a discontinuity around 76 GPa in the variation of the Fe–Mg solid/liquid partition coefficient of laser-heated olivine with pressure that they attributed to spin crossover in the melt. The sharpness of the discontinuity (width <3 GPa) and the relative invariance of partition coefficients with pressure extending on either side of the discontinuity would require complete spin crossover over a narrow pressure range. Such behaviour would imply not only negligible iron–iron interactions in the melt and minimal variation of coordination environments

between different iron atoms, but also virtually no thermal broadening of the width of the transition region (e.g., Kantor et al., 2009). Shock-wave data from a recent study of liquid Fe_2SiO_4 up to 161 GPa could be fit to a single Hugoniot (Thomas et al., 2012), suggesting either the absence of spin crossover or its occurrence over a wide pressure range. Andrault et al. (2012) performed partitioning experiments similar to those of Nomura et al. (2011), but used a chondritic-type material instead, and observed no discontinuity in the variation of solid/melt partition coefficient with pressure. Although their partition coefficients (K_D) were significantly higher (meaning that the chondritic melt is less iron-rich relative to the solid phases than the $(Mg,Fe)_2SiO_4$ melt at all pressures), the chondritic K_D values do show a linear decrease from 0.60(5) at 42 GPa to 0.47(5) at 120 GPa. This decrease means that the chondritic melt does become more Fe-rich with increasing pressure, possibly due to a coordination change in the melt that stabilizes a higher concentration of iron (e.g., Murakami and Bass, 2011). However, the data of Andrault et al. (2012) lack a discontinuity, indicating that no sharp spin crossover occurs in chondritic melts at depths of the Earth's lower mantle. The results of our Mössbauer spectroscopy investigation of the electronic behavior of Fe in glasses suggests that Fe^{2+} and Fe^{3+} will remain in the HS state in more complex Al- and Na-bearing melts. Hence the magnitude of Fe enrichment is not sufficient for a chondritic silicate melt to become negatively buoyant in the Earth's lower mantle (Andrault et al., 2012). Nevertheless, such Fe enrichment coupled with the structural changes in the Si polyhedron proposed by Murakami and Bass (2011) might be sufficient to generate negatively buoyant melts near the CMB (Stixrude and Karki, 2005; De Koker et al., 2013), which could explain the anomalies at the CMB seen by seismology (Williams and Garnero, 1996).

Acknowledgements

We acknowledge the European Synchrotron Radiation Facility for provision of synchrotron radiation (ID18) and we would like to thank Jean-Philippe Celse for additional technical assistance. The project was partly supported by funds from the German Science Foundation (DFG) through both the Priority Programme SPP1236 and a normal research grant, from the PROCOPE exchange programme, and from the German Federal Ministry for Education and Research (BMBF).

References

Agee, C.B., Walker, D., 1988. Static compression and olivine flotation in ultrabasic silicate liquid. J. Geophys. Res. 93, 3437–3449.

Agnor, C.B., Canup, R.M., Levison, H.F., 1999. On the character and consequences of large impacts in the late stage of terrestrial planet formation. Icarus 142, 219–237.

Andrault, D., Petitgirard, S., Nigro, G.L., Devidal, J.-L., Veronesi, G., Garbarino, G., Mezouar, M., 2012. Solid–liquid iron partitioning in Earth's deep mantle. Nature 487, 354–357.

Bengtson, A., Li, J., Morgan, D., 2009. Mössbauer modeling to interpret the spin state of iron in $(Mg,Fe)SiO_3$ perovskite. Geophys. Res. Lett. 36, 1–5.

Burns, R.G., 1993. Mineralogical Applications of Crystal Field Theory, second ed. Cambridge University Press, Cambridge, UK. 551 pp.

Catalli, K., Shim, S.-H., Prakapenka, V.B., Zhao, J., Sturhahn, W., Chow, P., Xiao, Y., Liu, H., Cynn, H., Evans, W.J., 2010. Spin state of ferric iron in $MgSiO_3$ perovskite and its effect on elastic properties. Earth Planet. Sci. Lett. 289, 68–75.

Catalli, K., Shim, S.-H., Dera, P., Prakapenka, V.B., Zhao, J., Sturhahn, W., Chow, P., Xiao, Y., Cynn, H., Evans, W.J., 2011. Effects of the Fe^{3+} spin transition on the properties of aluminous perovskite—New insights for lower-mantle seismic heterogeneities. Earth Planet. Sci. Lett. 310, 293–302.

De Koker, N., Karki, B.B., Stixrude, L., 2013. Thermodynamics of the $MgO–SiO_2$ liquid system in Earth's lowermost mantle from first principles. Earth Planet. Sci. Lett. 361, 58–63.

Dyar, M.D., 1985. A review of Mössbauer data on inorganic glasses: the effects of composition on iron valency and coordination. Am. Mineral. 70, 304–316.

Funamori, N., Sato, T., 2010. Density contrast between silicate melts and crystals in the deep mantle: An integrated view based on static-compression data. Earth Planet. Sci. Lett. 295, 435–440.

Gu, C., Catalli, K., Grocholski, B., Gao, L., Alp, E., Chow, P., Xiao, Y., Cynn, H., Evans, W.J., Shim, S.-H., 2012. Electronic structure of iron in magnesium silicate glasses at high pressure. Geophys. Res. Lett. 39, L24304.

Hearne, G.R., Pasternak, M.P., Taylor, R.D., Lacorre, P., 1995. Electronic structure and magnetic properties of $LaFeO_3$ at high pressure. Phys. Rev. B 51, 11495–11500.

Hsu, H., Blaha, P., Cococcioni, M., Wentzcovitch, R.M., 2011. Spin-state crossover and hyperfine interactions of ferric iron in $MgSiO_3$ perovskite. Phys. Rev. Lett. 106, 1–4.

Hsu, H., Yu, Y.G., Wentzcovitch, R.M., 2012. Spin crossover of iron in aluminous $MgSiO_3$ perovskite and post-perovskite. Earth Planet. Sci. Lett. 359–360, 34–39.

Ingalls, R., 1964. Electric-field gradient tensor in ferrous compounds. Phys. Rev. 133, A787–A793.

Jackson, J.M., Sturhahn, W., Shen, G., Zhao, J., Hu, M., Errandonea, D., Bass, J.D., Fei, Y., 2005. A synchrotron Mössbauer spectroscopy study of $(Mg,Fe)SiO_3$ perovskite up to 120 GPa. Am. Mineral. 90, 199–205.

Kantor, I., Dubrovinsky, L., McCammon, C., Steinle-Neumann, G., Kantor, A., Skorodumova, N., Pascarelli, S., Aquilanti, G., 2009. Short-range order in $Mg_{1-x}Fe_xO$ under high pressure. Phys. Rev. B 80, 014204.

Keppler, H., Rubie, D.C., 1993. Pressure-induced coordination changes of transition-metal ions in silicate melts. Nature 364, 54–56.

Kurnosov, A., Kantor, I., Boffa-Ballaran, T., Lindhardt, S., Dubrovinsky, L., Kuznetsov, A., Zehnder, B.H., 2008. A novel gas-loading system for mechanically closing of various types of diamond anvil cells. Rev. Sci. Instrum. 79, 045110.

Lagarec, K., Rancourt, D., 1997. Extended Voigt-based analytic lineshape method for determining *N*-dimensional correlated hyperfine parameter distributions in Mössbauer spectroscopy. Nucl. Instrum. Methods B 129, 266–280.

Lee, S.K., Lin, J., Cai, Y.Q., Hiraoka, N., Eng, P.J., Okuchi, T., Mao, H., 2008. X-ray Raman scattering study of $MgSiO_3$ glass at high pressure: Implication for triclustered $MgSiO_3$ melt in Earth's mantle. Proc. Natl. Acad. Sci. USA 105, 7925–7929.

Li, J., Sturhahn, W., Jackson, J.M., Struzhkin, V.V., Lin, J.F., Zhao, J., Mao, H.K., Shen, G., 2006. Pressure effect on the electronic structure of iron in $(Mg,Fe)(Si,Al)O_3$ perovskite: a combined synchrotron Mössbauer and X-ray emission spectroscopy study up to 100 GPa. Phys. Chem. Miner. 33, 575–585.

Lin, J.-F., Gavriliuk, A., Struzhkin, V., Jacobsen, S., Sturhahn, W., Hu, M., Chow, P., Yoo, C.-S., 2006. Pressure-induced electronic spin transition of iron in magnesiowüstite-(Mg,FeO). Phys. Rev. B 73, 73–76.

Lin, J.-F., Fukui, H., Prendergast, D., Okuchi, T., Cai, Y., Hiraoka, N., Yoo, C.-S., Trave, A., Eng, P., Hu, M., Chow, P., 2007. Electronic bonding transition in compressed SiO_2 glass. Phys. Rev. B 75, 1–4.

Mao, H.K., Xu, J., Bell, P.M., 1986. Calibration of the ruby pressure gauge to 800 kbar under quasi-hydrostatic conditions. J. Geophys. Res. 91, 4673–4676.

McCammon, C.A., 2000. Insights into phase transformations from Mössbauer spectroscopy. Rev. Mineral. Geochem. 39, 241–264.

McCammon, C., Kantor, I., Narygina, O., Rouquette, J., Ponkratz, U., Sergueev, I., Mezouar, M., Prakapenka, V., Dubrovinsky, L., 2008. Stable intermediate-spin ferrous iron in lower-mantle perovskite. Nat. Geosci. 1, 684–687.

Miller, G.H., Stolper, E.M., Ahrens, T.J., 1991. The equation of state of a molten Komatiite – shock wave compression to 36 GPa. J. Geophys. Res. 96, 11831–11848.

Murakami, M., Bass, J.D., 2010. Spectroscopic evidence for ultrahigh-pressure polymorphism in SiO_2 Glass. Phys. Rev. Lett. 104, 1–4.

Murakami, M., Bass, J.D., 2011. Evidence of denser $MgSiO_3$ glass above 133 gigapascal (GPa) and implications for remnants of ultradense silicate melt from a deep magma ocean. Proc. Natl. Acad. Sci. USA 108, 17286–17289.

Nomura, R., Ozawa, H., Tateno, S., Hirose, K., Hernlund, J., Muto, S., Ishii, H., Hiraoka, N., 2011. Spin crossover and iron-rich silicate melt in the Earth's deep mantle. Nature 473, 199–202.

Ohtani, E., Maeda, M., 2001. Density of basaltic melt at high pressure and stability of the melt at the base of the lower mantle. Earth Planet. Sci. Lett. 193, 69–75.

Pasternak, M.P., Xu, W.M., Rozenberg, G.K., Taylor, R.D., 2002. Electronic, magnetic and structural properties of the $RFeO_3$ antiferromagnetic-perovskites at very high pressures. Mater. Res. Soc. Symp. Proc. 718, D2.7.1–D2.7.10.

Potapkin, V., Chumakov, A.I., Smirnov, G.V., Celse, J.P., Rüffer, R., McCammon , C., Dubrovinsky, L., 2012. The ^{57}Fe synchrotron Mössbauer source at the ESRF. J. Synchrotron Radiat. 19, 559–569.

Prescher, C., McCammon, C., Dubrovinsky, L., 2012. MossA: a program for analyzing energy-domain Mössbauer spectra from conventional and synchrotron sources. J. Appl. Crystallogr. 45, 329–331.

Rigden, S.M., Ahrens, T.J., Stolper, E.M., 1984. Densities of liquid silicates at high pressures. Science 226, 1071–1074.

Rouquette, J., Kantor, I., McCammon, C.A., Dmitriev, V., Dubrovinsky, L.S., 2008. High-pressure studies of olivine $(Mg_{0.9}Fe_{0.1})_2SiO_4$ using Raman spectroscopy, X-ray diffraction and Mössbauer spectroscopy. Inorg. Chem. 47, 2668–2673.

Rüffer, R., Chumakov, A.I., 1996. Nuclear resonance beamline at ESRF. Hyperfine Interact. 97/98, 589–604.

Sarkisyan, V.A., Troyan, I.A., Lyubutin, I.S., Gavrilyuk, A.G., Kashuba, A.F., 2002. Magnetic collapse and the change of electronic structure of $FeBO_3$ antiferromagnet under high pressure. JETP Lett. 76, 664–669.

Sato, T., Funamori, N., 2008. Sixfold-coordinated amorphous polymorph of SiO_2 under high pressure. Phys. Rev. Lett. 101, 1–4.

Shim, S.-H., Catalli, K., 2009. Compositional dependence of structural transition pressures in amorphous phases with mantle-related compositions. Earth Planet. Sci. Lett. 283, 174–180.

Stixrude, L., Karki, B., 2005. Structure and freezing of $MgSiO_3$ liquid in Earth's lower mantle. Science 310, 297–299.

Thomas, C.W., Liu, Q., Agee, C.B., Asimow, P.D., Lange, R.A., 2012. Multi-technique equation of state for Fe_2SiO_4 melt and the density of Fe-bearing silicate melts from 0 to 161 GPa. J. Geophys. Res. 117, B10206.

Tonks, W.B., Melosh, H.J., 1993. Magma ocean formation due to giant impacts. J. Geophys. Res. 98, 5319–5333.

Weigel, C., Cormier, L., Calas, G., Galoisy, L., Bowron, D.T., 2008. Nature and distribution of iron sites in a sodium silicate glass investigated by neutron diffraction and EPSR simulation. J. Non-Cryst. Solids 354, 5378–5385.

Williams, Q., Garnero, E.J., 1996. Seismic evidence for partial melt at the base of Earth's mantle. Science 273, 1528–1530.

Xu, W.M., Naaman, O., Rozenberg, G.K., Pasternak, M.P., Taylor, R.D., 2001. Pressure-induced breakdown of a correlated system: The progressive collapse of the Mott–Hubbard state in $RFeO_3$. Phys. Rev. B 64, 094411. 9 pp.

Zha, C., Hemley, R.J., Mao, H., Duffy, T.S., Meade, C., 1994. Acoustic velocities and refractive index of SiO_2 glass to 57.5 GPa by Brillouin scattering. Phys. Rev. B 50, 13105–13112.